An Investigation of the Structure of Amorphous Co-P Alloys. 1: X-ray and Neutron Diffraction

Mi. Nuding, P. Lamparter, and S. Steeb

Max-Planck-Institut für Metallforschung, Seestr. 92, D-70174 Stuttgart

Z. Naturforsch. **53 a,** 841–847 (1998); received September 12, 1998

Amorphous Co-P alloys with different phosphorous concentrations were produced by melt-spinning, sputtering, and electrodeposition. From the combination of X-ray and neutron diffraction the atomic distances and coordination numbers for the Co-Co- and the Co-P correlations were determined. The short range structure, in dependence of the P-concentration, 9 at% P $\leq c_p \leq$ 26 at% P, exhibits rather abrupt changes at the eutectic composition, $c_{p,e}$ = 19.9 at% P. It is suggested that at P-contents above $c_{p,e}$ the short range order is more pronounced than at lower P-contents. The coordination of nine Co atoms around P, as established previously for many transition metal-metalloid glasses, is found only at the eutectic composition. There is almost no dependence of the structure of the amorphous alloys on the specific production method. It is indicated that the melt-spun and the sputtered glasses are in a slightly more relaxed state than the electrodeposited glasses.

1. Introduction

Amorphous binary Co-P alloys are rather good soft magnetic construction materials [1] with excellent corrosion resistance versus oxygen-, chloride-, nitrate-, sulfate-, and sulfite-containing environments [2 - 7]. They seem to be suitable for the production of thin film video heads and memory devices because of their rather high magnetic coercitive field strength [8 - 14].

Investigations of the structure of Co-P metallic glasses and other metal-metalloid alloys have been reported already by several authors. In Table 1 we present a compilation of structural data of amorphous transition metal (Fe, Co, Ni)-phosphorous alloys from previous studies. However, very few detailed investigations of the dependence of the structure on the metalloid content have been performed. It has been suggested that the coordination of nine metal atoms around one metalloid atom is a rather stable configuration, which does not depend on the composition (see e. g. [25]). In fact, the values of Z_{P-TM} in Table 1 seem to support this suggestion.

In the present work (Part 1) the compositional dependence of the structure of $Co_{100-x}P_x$ metallic glasses was investigated within the range $9 \leq x \leq 26$, employing the combination of X-ray and neutron diffraction. Furthermore, we studied the dependence of the structure on different methods for the production of amorphous Co-P alloys: melt-spinning, electrodeposition, and sputtering. In the following paper (Part 2) [26] an EXAFS study of amorphous Co-P alloys will be presented.

Concerning the principles of X-ray- and neutron-diffraction with amorphous alloys we refer to the review [25] and the references therein. In the present work the definitions of structural parameters and the symbols from [25] were used.

Table 1. Amorphous transition metal (TM)-phosphorous (P) glasses: atomic distances R_{i-j} and partial coordination numbers Z_{i-j}. X: X-ray diffraction, n: neutron diffraction, TOF: time of flight spectroscopy, pol: polarized neutrons, DRP: dense random packing.

Alloy	Ref.	R_{TM-TM} [Å]	R_{P-TM} [Å]	Z_{TM-TM}	Z_{P-TM}	Method
$Co_{80.0}P_{20.0}$	here	2.54	2.30	11.5	9.2	X, n
$Co_{81.8}P_{18.2}$	[15]	2.57	2.30	10.0	8.0	n TOF
$Co_{80.0}P_{20.0}$	[16]	2.55	2.32	10.1	8.9	n pol
$Co_{80.0}P_{20.0}$	[17]	2.47	2.29	10.5	—	Co-K EXAFS
$Co_{80.0}P_{20.0}$	[17]	—	2.29	—	9.0	P-K EXAFS
$Co_{76.0}P_{24.0}$	[18]	2.64	2.28	10.0	—	Co-K EXAFS
$Co_{66.0}P_{34.0}$	[19]	2.48	2.20	9.0	—	Co-K EXAFS
$Co_{66.0}P_{34.0}$	[19]	—	2.20	—	9.0	P-K EXAFS
$Ni_{80.0}P_{20.0}$	[20]	2.56	2.28	9.4	9.3	n
$Fe_{85.0}P_{15.0}$	[21]	2.60	2.28	11.2	9.1	DRP model
$Fe_{82.0}P_{18.0}$	[22]	2.61	2.38	10.7	8.1	X
$Fe_{80.0}P_{20.0}$	[23]	—	—	10.2	8.4	DRP model
$Fe_{80.0}P_{20.0}$	[24]	2.61	2.32	10.0	—	Fe-K EXAFS

Reprint requests to Dr. P. Lamparter; Fax: +49 711 2095420.

0932–0784 / 98 / 1000–0841 $ 06.00

2. Experimental

2.1. Sample Preparation

Three different methods for the preparation of the amorphous Co-P alloys were used, namely melt-spinning (MS), sputtering (SP), and electrodeposition (ED).

2.1.1. Melt-spinning

From pieces and powder of cobalt (99.99 %) and from pieces of phosphorous (99.9999 %) small cylinders were obtained by pressing. The cylinders were filled into quartz tubes which were sealed under argon atmosphere. At a temperature of 580 °C the phosphorous forms the Co_2P compound and the cylinders then consist of Co_2P together with metallic Co. These cylinders were melted by induction heating under argon (p = 400 mbar) and then cast into a copper mould.

Deep eutectica and different atomic radii of the constituents favour the formation of amorphous metal-metalloid alloys during rapid quenching. The Co-P phase diagram [27] shows a deep minimum at $c_{p,e}$ = 19.9 at% P. $Co_{100-x}P_x$ alloys with x = 14, 16, 18, 20, 22, 24, and 26 were used to produce ribbons with a melt spin apparatus. The alloys with x = 20, 22, and 24 yielded amorphous ribbons (breadth: 1 mm; thickness: 15 μm; length: several meters), whereas the other alloys yielded only small pieces which were partly crystalline.

2.1.2. Sputtering

$Co_{100-x}P_x$ targets with the concentrations x = 20, 24, and 26 were produced by induction melting from metallic cobalt and Co_2P powder. The most suitable sputter parameters for the production of amorphous films were a pressure of 8×10^{-3} Torr argon (5N), 0.12 A cathode current, 1.20 kV high frequency potential, and a DC-potential of 1.10 kV. The sputter yield was 12 mg/h corresponding to a growth in thickness of 0.42 μm/h. Aluminum foil was used as substrate and then dissolved by a NaOH solution at 40 °C in order to obtain self supporting films.

2.1.3. Electrodeposition

Using the method of electrodeposition, amorphous $Co_{100-x}P_x$ alloy films can be produced in a wide concentration range [28, 29]. We used as cathode a polished and degreased Cu-foil with a free surface of 32×32 mm² and as anode a cylinder of cobalt (99.99 %). Electrolyte compositions were used as described in [29].

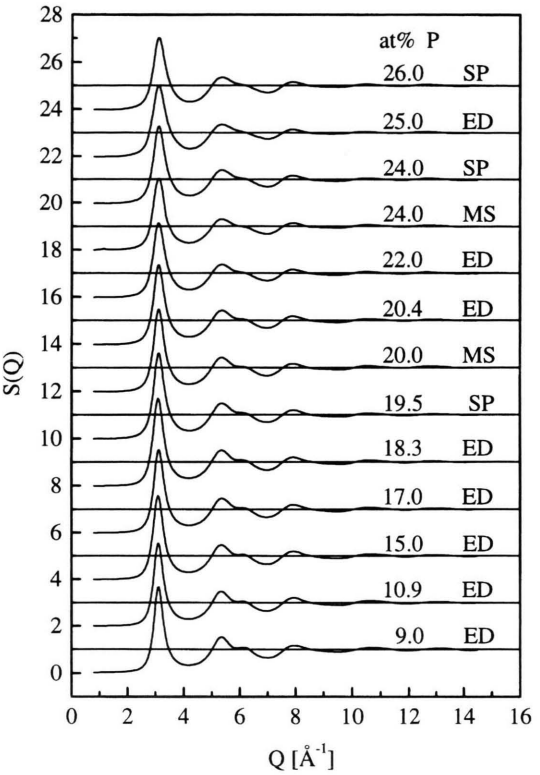

Fig. 1. Amorphous Co-P: total structure factors from X-ray diffraction. MS: melt spun, SP: sputtered, ED: electrodeposited.

2.2. Diffraction Experiments

X-ray diffraction was done with a goniometer (Siemens D500) in transmission mode using a primary beam monochromator for Mo-Kα-radiation and a position-sensitive detector. The corrections for polarization, absorption, incoherent scattering, and multiple scattering as well as the normalization procedure were done as described in [29]. Neutron diffraction was done in transmission mode using the instrument D20 at the Institute Laue Langevin (Grenoble) and the instrument 7C2 at the Laboratoire Léon Brillouin (Saclay). For the diffraction experiments between 3 and 5 g of the amorphous alloys were cut into small pieces and filled into vanadium-containers. The usual corrections for counter efficiency, background, absorption, multiple scattering, inelastic scattering as well as the normalization procedure were done as described in [29]. From the diffraction data the total

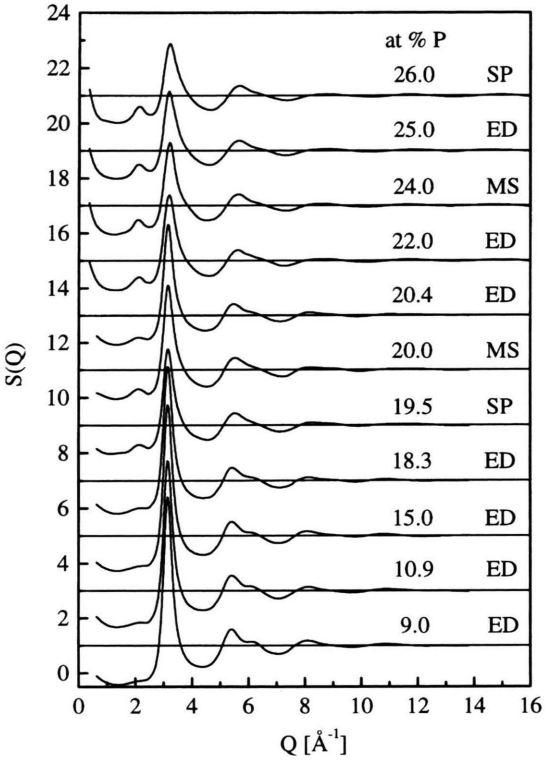

Fig. 2. Amorphous Co-P: total structure factors from neutron diffraction. $9 < x < 20.4$: instrument D20, ILL, λ = 0.879 Å. $22 < x < 26$: instrument 7C2, LLB, λ = 0.70 Å.

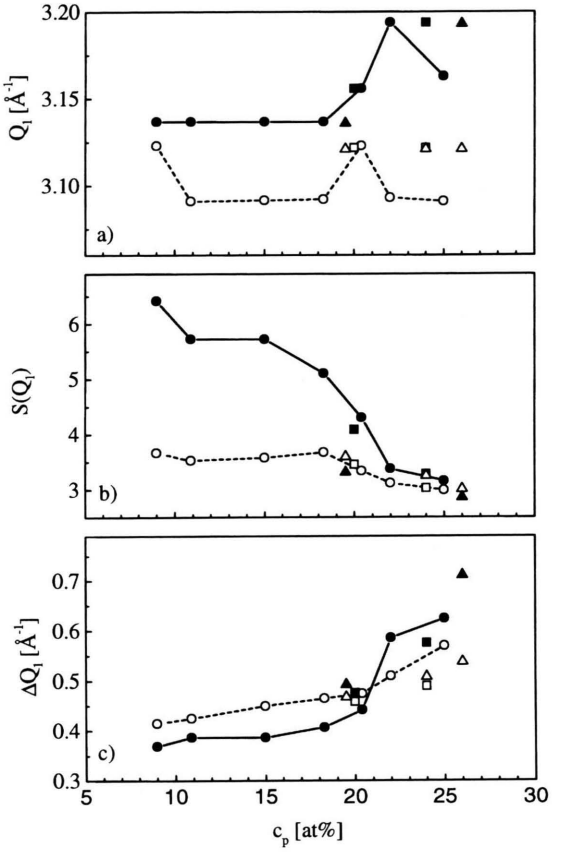

Fig. 3. Amorphous Co-P: characteristic parameters of the main peak of the total structure factors in Figs. 1 and 2. Q_1: position, $S(Q_1)$: height, ΔQ_1: width. Open symbols: X-rays, full symbols: neutrons. o: electrodeposited, Δ: sputtered, □: melt spun. The lines are drawn for the ED-samples as guide to the eye.

structure factors were calculated according to the Faber-Ziman notation [25].

3. Results and Discussion

3.1. Total Structure Factors

The total structure factors $S(Q)$ of the Co-P alloys as obtained by X-ray diffraction and by neutron diffraction are plotted in Figs. 1 and 2 versus the momentum transfer $Q = 4\pi(\sin\theta)/\lambda$, where 2θ is the scattering angle and λ is the wavelength. In Fig. 3 the characteristic parameters of the main peak of the structure factors are shown in dependence of the P-concentration. Although these parameters do not provide a direct insight into the structure, they are very sensitive for structural changes. It is interesting to note that these changes, due to the increasing P-content, do not take place gradually but rather abruptly close to the eutectic composition of the Co-P system, $c_{p,e}$ = 19.9 at%.

The neutron $S(Q)$ in Fig. 2 exhibit a prepeak at Q_P = 2.1 Å^{-1}. As this peak does not occur in the X-ray $S(Q)$ in Fig. 1 and as its amplitude increases with increasing P-content, we can conclude that it is caused by P-P pairs which are not directly neighboured, but are separated by Co-atoms. The common view of this phenomenon is that the chemical interaction between the metal- and the metalloid atoms causes a chemical short range order effect which is characterized by a shell of Co-atoms around a central P-atom [25]. If we discuss this structural feature in terms of concentration fluctuations, i. e. as a deviation from a statistical distribution of the Co- and P-atoms, it is interesting to note that X-ray diffraction is not sensitive to concentration fluctuations. This is due to the fact that the Co- and the P-atoms exhibit nearly equal

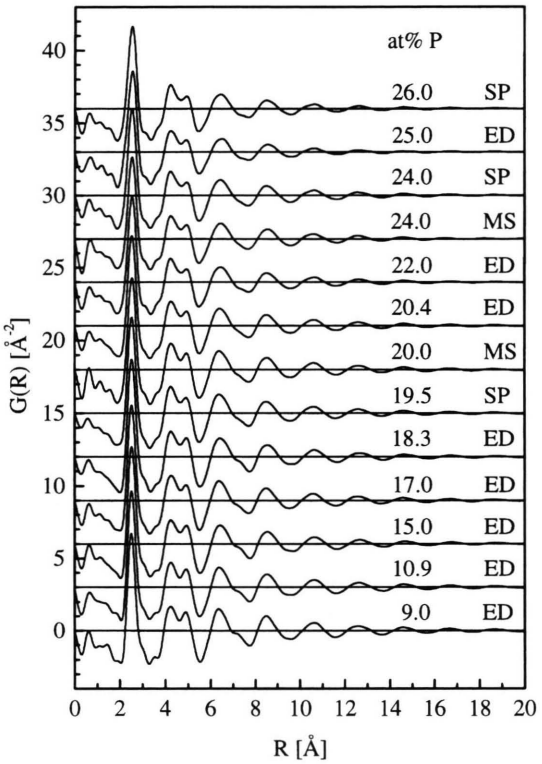

Fig. 4. Amorphous Co-P: total pair correlation functions from X-ray diffraction.

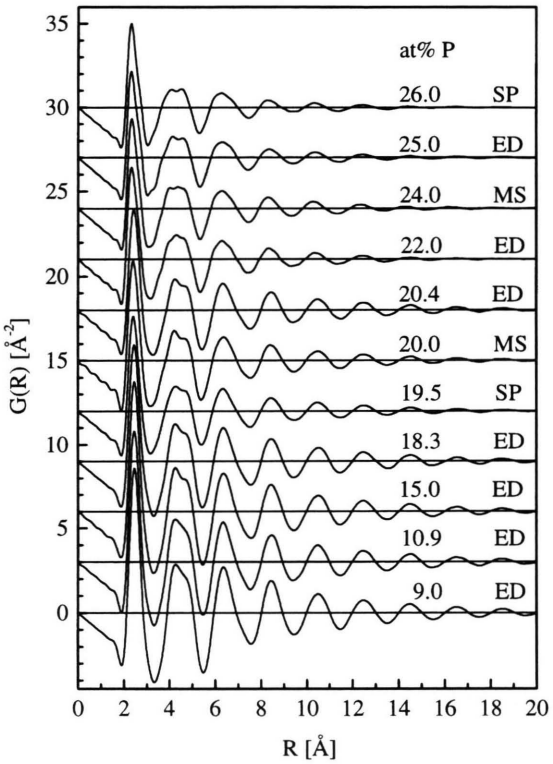

Fig. 5. Amorphous Co-P: total pair correlation functions from neutron diffraction.

electron densities in the amorphous alloys, i. e. their atomic volume scales roughly with their atomic number. In contrast, for neutrons the scattering length of the smaller P-atoms ($b_P = 0.51 \times 10^{-12}$ cm) is larger than that of the Co-atoms ($b_{Co} = 0.25 \times 10^{-12}$ cm), which means that concentration fluctuations give rise to fluctuations of the scattering length density.

These considerations are revealing for a second interesting feature in Figure 2. With neutrons we observe a small angle scattering effect which does not appear with X-rays (Figure 1). Obviously, this effect is caused by concentration fluctuations. It is suggested that some kind of chemically ordered Co-P clusters exist in the Co-P glasses. From the onset of the small angle scattering effect around $Q \leq 1$ Å^{-1} the size of the clusters can be roughly estimated to be in the order of 10 Å, which corresponds to one shell of Co atoms around a central P atom. For a quantitative investigation of this structural behaviour dedicated small angle scattering experiments, including the magnetic scattering, are required.

3.2. Total Pair Correlation Functions

The total pair correlation functions $G(R)$, as obtained by Fourier transformation of the $S(Q)$-functions, are shown in Figs. 4 and 5. These total functions are composed of three partial pair correlation functions $G_{ij}(R)$. For the case of the composition $Co_{80}P_{20}$ and neglecting the magnetic scattering contributions:

$$G^{X}(R) = 0.77\, G_{CoCo}(R) + 0.02\, G_{PP}(R) + 0.21\, G_{CoP}(R), \tag{1a}$$

$$G^{n}(R) = 0.44\, G_{CoCo}(R) + 0.11\, G_{PP}(R) + 0.45\, G_{CoP}(R). \tag{1b}$$

The weighting factors of the partial $G_{ij}(R)$ show a distinct contrast between X-rays and neutrons. With X-rays the total $G(R)$ is mainly determined by the partial $G_{CoCo}(R)$-function. Furthermore, for X-rays the contribution of $G_{PP}(R)$ can be neglected and for neutrons it is rather small.

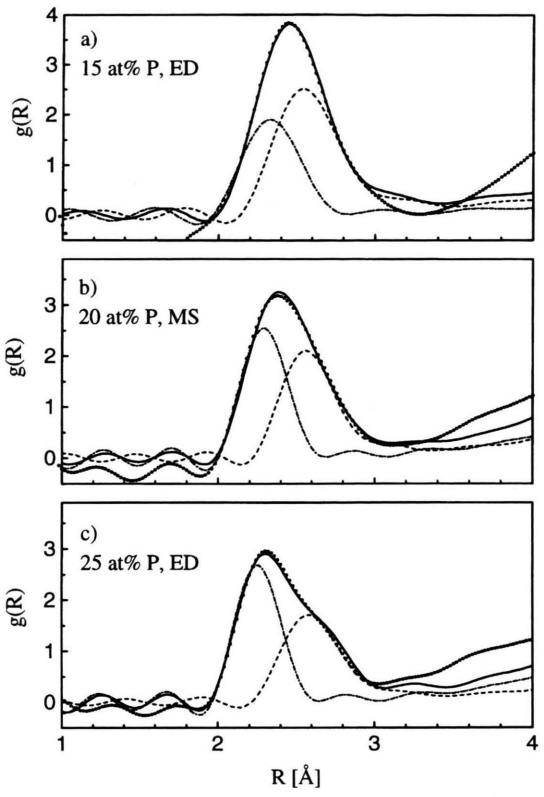

Fig. 6. Amorphous Co-P: fit of the main peak of $g(R)$ (see text). — experimental curve from neutron diffraction, • fit, - - - contribution of $g_{CoCo}(R)$, - · - contribution of $g_{CoP}(R)$.

3.3. *Evaluation of the Co-Co and Co-P Partial Correlations*

The straightforward derivation of the three partial correlation functions from only two independent scattering experiments is not possible. Therefore we used an alternative approach to determine the Co-Co and the Co-P partial correlations within the range of their first coordination shells. This is based on the facts that the overall contribution of the P-P correlations to the total $G(R)$ is small (1a and b) and, in particular, that in the range of the first coordination shell around the P-atoms the contribution of P-P atomic pairs, not appearing as direct neigbours, can be neglected.

Different techniques to obtain $G_{CoCo}(R)$ and $G_{CoP}(R)$ from the total $G^X(R)$ and $G^n(R)$ were tested. Their direct calculation from (1a and b) by neglecting $G_{PP}(R)$, yielded partial $G_{ij}(R)$ from which the atomic distances R_{CoCo} and R_{CoP} were obtained. However, the resulting coordination numbers seemed to be questionable [29]. More reasonable results were obtained by fitting partial functions, $g_{CoCo}(R)$ and $g_{CoP}(R)$, to the total $g(R)$ functions. Note, that $g_{ij}(R)$-functions and $G_{ij}(R)$-functions are related by

$$G_{ij}(R) = 4\pi\rho_0 R[g_{ij}(R) - 1], \tag{2}$$

where ρ_0 is the mean atomic density.

Usually Gaussian curves are employed for this type of analysis. As a better method, we used the partial correlation functions $g_{NiNi}(R)$ and $g_{NiP}(R)$ which have been established for the $Ni_{80}P_{20}$ glass by neutron diffraction using the isotopic substitution technique [20]. It is supposed that the characteristic features of these functions are the same in the systems Ni-P and Co-P, in particular their asymmetric shape. During the computer fits, the position, the amplitude, and the width of the main peak of the input functions $g_{NiNi}(R)$ and $g_{NiP}(R)$ were varied as parameters. The examples of the fitting procedure to the neutron $G^n(R)$, shown in Fig. 6, illustrate the good agreement between the experimental and the fitting curves.

The nuclear scattering lengths $b_{Co} = 0.253\times10^{-12}$ cm and $b_P = 0.513\times10^{-12}$ cm were used for the calculation of the weights for the Co-Co and the Co-P contributions. An estimation of the magnetic contribution of the Co-Co pairs, according to the methods as described e. g. in [30, 31], showed that it is very small within the range of the first coordination shell. Therefore it was neglected during the fitting procedure.

The structural parameters for the Co-Co and the Co-P correlations from the fits are presented in Fig. 7 in dependence of the P-concentration. An overview shows that the composition at 20 at% P, where the phase diagram of the Co-P system has an eutectic point ($c_{p,e}$ = 19.9 at% P), is a particular one. With increasing P-content there are pronounced variations at the point $c_{p,e}$ which may be even quite abrupt. The distance between the Co-atoms, R_{CoCo}, increases, where a steeper increase is indicated above $c_{p,e}$. At P-concentrations above $c_{p,e}$ a higher degree of order in the amorphous alloys is indicated: The distance R_{CoP} exhibits a distinct contraction and the widths of the Co-P and Co-Co bond lengths, ΔR_{CoP} and ΔR_{CoCo}, become sharper. At the same time, the decrease of the coordination number Z_{CoCo} exhibits a jump at $c_{p,e}$ by about two Co-atoms. An important result in Fig. 7 is that the number of Co-atoms around P decreases from Z_{PCo} = 10.5 to Z_{PCo} = 8 over the investigated range of the P-concentration. This finding is contradictory to previous works, where the number of 9 metal atoms

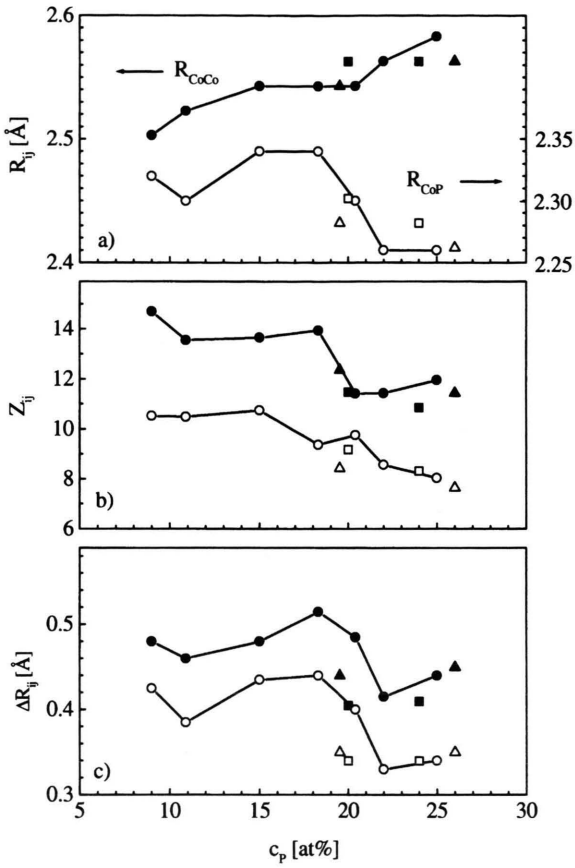

Fig. 7. Amorphous Co-P: structural parameters for the Co-Co (full symbols) and the Co-P (open symbols) correlations. R_{ij}: atomic distance, Z_{ij}: coordination number, ΔR_{ij}: width of bond length distribution. ○: electrodeposited, △: sputtered, □: melt spun. The lines are drawn for the ED-samples as guide to the eye.

around a metalloid atom in T-M glasses has been suggested as a stable structural feature, independent from the metalloid content [25]. The coordination number $Z_{PCo} = 9$ is found in the present work only around the eutectic composition.

3.4. Dependence on the Method of Preparation

Figures 1 and 2 contain the structure factors $S(Q)$ of three samples close to the eutectic composition, which were produced by different methods: sputtered $Co_{80.5}P_{19.5}$(SP), melt spun $Co_{80}P_{20}$(MS), and electrodeposited $Co_{79.6}P_{20.4}$ (ED).

The nearly equal structure factors indicate that the structure of the amorphous Co-P alloys does not depend on the preparation method. Considering that the formation of the amorphous solid is very different during the three methods, namely atom by atom from the gas phase (SP) or from the liquid (ED) or, finally, solidification of a system of atoms which are already in close contact (MS), the uniqueness of the resulting structure is by no means evident. Apparently, the chemical interaction between the metal- and the metalloid atoms causes a well defined amorphous structure.

However, the very details of the structure show some differences. The prepeak at $Q_P = 2.1$ Å^{-1} in Fig. 2 is less pronounced for the ED-sample than for the MS- and the SP-sample. This indicates that the distance correlations between the P-atoms are somewhat less defined in the ED-sample. The widths of the Co-Co- and of the Co-P bond length distributions, at $c_{p,e}$ in Fig. 7c, are larger for the ED-sample, which again reflects a lower degree of order in the electrodeposited material. It is suggested that during the consolidation of the amorphous alloys the freedom for the relaxation into an ordered metastable state is higher during the melt-spinning process and the sputter process than during the electrodeposition process.

4. Conclusions

Amorphous Co_xP_{100-x} alloys with $9 < x < 26$ were produced by electrodeposition, melt-spinning and sputtering. The concentration dependence of their structure was investigated by X-ray- and neutron diffraction. The atomic order is governed by the chemical interaction between the metal- and the metalloid atoms, which generates a Co-shell around the P-atoms. With increasing P-content the Co-Co distance increases, whereas the Co-P-distance decreases. At the eutectic concentration (19.9 at% P) pronounced variations occur, and a more ordered structure is indicated above this concentration. As the number of Co atoms around P decreases with increasing P-content from $Z_{PCo} = 10.5$ to $Z_{PCo} = 8$, the view of ninefold coordination of the P-atoms as a concentration-independent structural feature is not confirmed. The influence of the different production methods on the structure is very small. The amorphous $Co_{80}P_{20}$-alloys produced by melt-spinning and by sputtering show slightly more pronounced Co-Co- and Co-P-pair distribution functions than those produced by electrodeposition.

Acknowledgements

Thanks are due to ILL, Grenoble and to LLB, Saclay for allocation of neutron beam time. This work was supported by the Deutsche Forschungsgemeinschaft through grant La 686/1.

[1] H. Fahlenbrach, Elektrotechnik **58**, 14 (1976).
[2] B. Gillot, K.E. Amri, P. Pouderoux, J.P. Bonino, and A. Rousset, J. of Alloys and Compounds **189**, 151 (1992).
[3] M. Naka, K. Hashimoto, and T. Masumoto, J. Japan. Inst. Metals **38**, 835 (1974).
[4] M. Naka, K. Hashimoto, and T. Masumoto, Corrosion **32**, 146 (1976).
[5] H. Jones, J. Mat. Sci. **19**, 1043 (1984).
[6] S. Virtanen and H. Boehni, ISIJ International **31**, 229 (1991).
[7] A. Kawashima, K. Asami, and K. Hashimoto, J. Non-Cryst. Solids **70**, 69 (1985).
[8] H. Tanaka, H. Goto. N. Shiota, and M. Yanagisawa, J. Appl. Phys. **53**, 2576 (1982).
[9] O. Kohmoto and T. Yamamoto, J. Magn. Mat. **71**, 33 (1987).
[10] J. Przyluski and M. Tomsia, IEEE Trans. Magn. **20**, 830 (1984).
[11] C.D. Wu, MRL Bull. Res. Dev. **4**, 59 (1990).
[12] L. Zhihui, C. Haoming, Y. Chen, and H. Yusheng, J. Phys.: Cond. Matter **3**, 9007 (1991).
[13] E.L. Nicholson and M.R. Khan, J. Electrochem. Soc. **133**, 2342(1986).
[14] T. Chen, D.A. Rogowski, and R.M. White, J. Appl. Phys. **49**, 1816 (1978).
[15] K. Suzuki and T. Fukunaga, Sci. Rep. RITU **10**, 209 (1977).
[16] J.F. Sadoc and J. Dixmier, Mat. Sci. Eng. **23**, 187 (1976).
[17] P. Lagarde, J. Rivory, and G. Vlaic, J. Non-Cryst. Solids **57**, 275 (1983).
[18] G.S. Cargill III, Proc. 4th Int. Conf. on Rapidly Quenched Metals, RQM4, Physical Soc. of Japan, Sendai, Japan 1981, p. 389.
[19] P. Lagarde, D. Raoux, and A. Fontaine, Proceedings of the Daresbury Weekend: EXAFS for Inorganic Systems, edts.: C.D. Garner and S.S. Hasnain, S.R.C. Daresbury Laboratory 1981, p. 122.
[20] P. Lamparter and S. Steeb, Proc. 5th Int. Conf. on Rapidly Quenched Metals, RQM5, North Holland Publ. Corp., edts. S. Steeb and H. Warlimont, Amsterdam 1985, p. 459.
[21] T. Fujiwara and Y. Ishii, J. Phys. F: Met. Phys. **10**, 1901 (1980).
[22] Y. Waseda and H.S. Chen, phys. stat. sol. (1) **49**, 387 (1978).
[23] D.S. Boudreaux, Phys. Rev. **B18**, 4039 (1978).
[24] A. Defrain, L. Bosio, R. Cortes, and P. Costa, J. Non-Cryst. Solids **61&62**, 439 (1984).
[25] P. Lamparter and S. Steeb, in: Materials Science and Technology, Vol. 1, ed. V. Gerold, VCH, Weinheim 1993, p. 217.
[26] Mi. Nuding, P. Lamparter, S. Steeb, F. Neißendorfer, and F. Schäfers, Z. Naturforsch. **53a**, 848 (1998).
[27] K. Ishida and T. Nishizawa, Bulletin of Alloy Phase Diagrams **11**, 555 (1990).
[28] G. Dietz, K. Richter, F. Stein, and H.C. Schäfer, Z. Phys. B, Condensed matter, **81**, 223 (1990).
[29] Mi. Nuding, thesis work, University of Stuttgart (1993).
[30] P. Lamparter, E. Nold, G. Rainer-Harbach, E. Grallath, and S. Steeb, Z. Naturforsch. **36a**, 165 (1981).
[31] E. Nold, P. Lamparter, H. Olbrich, G. Rainer-Harbach, and S. Steeb, Z. Naturforsch. **36a**, 1032 (1981).